LRP 579/97 August 1997

TOROIDAL MODE-CONVERSION IN THE ICRF

A. Jaun, T. Hellsten, S.C. Chiu

Annex:

Ion-Bernstein Wave Mode-Conversion in Hot Tokamak Plasmas
A. Jaun, T. Hellsten, S.C. Chiu
12th Topical Conf. on RF power in Plasmas, Savannah - 1997

submitted for publication to
Nuclear Fusion

Toroidal Mode-Conversion in the ICRF

A. Jaun[1,2], T. Hellsten[1], S. C. Chiu[3]

[1] Alfvén Laboratory, EURATOM-NFR Association, KTH, 100 44 Stockholm, Sweden
[2] CRPP-EPFL, Association Euratom-Confédération Suisse, 1015 Lausanne, Switzerland
[3] General Atomics, San Diego, California 92186-9784, USA

ABSTRACT. Mode-conversion is studied in the ion-cyclotron range of frequencies (ICRF) taking into account the toroidal geometry relevant for tokamaks. The global wavefields obtained using the gyrokinetic toroidal PENN code illustrate how the fast wave propagates to the neighborhood of the ion-ion hybrid resonance, where it is converted to a slow wave which deposits the wave energy through resonant interactions with the particles. The power deposition profiles obtained are dramatically different from the toroidal resonance absorption, showing that Budden's model is not a good approximation in the torus. Radially and poloidally localized wavefield structures characteristic of slow wave eigenmodes are predicted and could in experiments be driven to large amplitudes so as to interact efficiently with fast particles.

a reminder in sect.2 of the principles behind the physical phenomenon, all three models used in the paper are briefly described with their possibilities and limitations. A DIII-D equilibrium is then analyzed in sect.3 for a mode-conversion scenario, showing that toroidal and kinetic effects are both important, and that toroidicity can strongly increase the efficiency of the mode conversion. A summary and some concluding remarks are given in sect.4.

2 MODELS

When waves in a physical system propagate somewhere with neighboring frequencies and wavevectors, the energy associated with one of the branches can be transferred to another in a process commonly called linear mode-conversion [9]. This generally occurs in the vicinity of fast wave resonances and slow wave cut-offs [9, 27] where the wavelengths undergo rapid variations due to the inhomogeneities in the plasma parameters; mode-conversion may also be induced non-resonantly by confluences [28, 29], toroidicity [30] and changes in the magnetic shear [31].

In the tokamak, the conversion taking place at the ion-ion hybrid resonance is intrinsically a two-dimensional gyrokinetic problem. It is two-dimensional because the flux-surface symmetry implied by the Alfvén resonances [21, 32] is broken by the vertical character of the cyclotron resonances. That it is kinetic is at the same time trivial, since the converted slow waves owe their mere existence to the particles finite gyro-orbits, and subtle because the mode-converted power can for a single resonance in slab geometry be evaluated with resonance absorption, which does not take into account the propagation of the slow wave at all. In this paper, three different models are used to analyze the same scenario:

- the gyrokinetic slab ISMENE-IV code [13, 14] solves the global wave equations in real space using 1-D cubic finite elements to discretize all three components of the electric field $(E_n, E_b, E_{||})$; the projections are "normal" to the surfaces with constant density and temperature, "parallel" to the magnetic field and "bi-normal" to the other two. The equilibrium profiles are chosen for a cross-section in the mid-plane and the plasma response defined using a second order FLR expansion of the dielectric tensor [33]. The power absorption may be separated locally from the kinetic power flux following Ref.[34, 35, 36]. In this form, the code describes the propagation, damping and mode conversion of global fast and slow waves in a slab plasma, with a power absorption due to resonant Landau, cyclotron and transit-time magnetic pumping (TTMP) interactions.

- The fluid toroidal LION code [19] solves the wave equations in real space using 2-D hybrid finite elements to avoid "numerical pollution", in terms of only two electric field components (E_n, E_b) that are perpendicular to the local magnetic field. Using a toroidal equilibrium [37], the *lukewarm* dielectric tensor of the plasma is defined so as to take into account the parallel dynamics of the particles, using the fast wave dispersion relation to evaluate the higher harmonic cyclotron damping and relying on resonance absorption to regularize the singularities in the fluid wave equations [38]. The power absorption can be derived from the anti-Hermitian part of the

dielectric tensor or through the divergence of the Poynting flux, enabling a local self-consistency check of the numerical solution. As shown in ref.[21], the contribution from the resonance absorption may however not be split among different species. In this form, the code describes the propagation and damping of global fast and shear Alfvén waves in a tokamak, with a power absorption induced by resonant Landau, cyclotron and TTMP interactions, plus a contribution from the resonance absorption.

- The relatively new gyrokinetic toroidal PENN code [23] has first been tested in different limiting cases where simplified models are available [23] and has been used since for toroidal mode-conversion studies to ion-drift [39], kinetic Alfvén [30] and ion-Bernstein waves [40]. Detailed comparisons have been carried out with global Alfvén eigenmode experiments: they show that excellent agreement is achieved between the wavefield [41] and the damping rates [31] predicted, and the measurements from the JET tokamak. The code solves the wave equations in real space using a bi-cubic finite elements representation in terms of the electromagnetic potentials $(A_n, A_b, A_{||}, \phi)$ avoiding the "numerical pollution" [23, 42]. Using the same toroidal equilibrium [37] as in LION, the dielectric tensor operator of the plasma response is defined using a second order FLR expansion of the dielectric tensor [43]. To evaluate analytically the velocity integrals over the resonant denominators $(\omega - l\Omega - k_{||}v_{||})^{-1}$, an approximate functional dependence $k_{||} = n/R$ is assumed instead of using the exact operator $k_{||} = -iB^{-1}\ \vec{B}\cdot\nabla$, where ω stands for the frequency, $l\Omega$ a multiple of the cyclotron harmonic, n the toroidal mode number, R the major radius and $k_{||}$ the wave-vector along the local magnetic field $\vec{B}$. By measuring $k_{||}$ directly on the wavefield, an iterative procedure may be used to make the calculation self-consistent [23]. The local power absorption calculated within the drift-kinetic approximation in eqs. 50-51 of Ref.[44] is completed with the corresponding first and second harmonic cyclotron absorption [45]:

$$P_{cycl} = \sqrt{\pi}\epsilon_0 \int d^3x \frac{\omega_p^2}{4|k_{||}|v_{th}} \left(|E_+|^2 \exp\left[-\left(\frac{\omega - \Omega}{k_{||}v_{th}} \right)^2 \right] + \rho_L^2 |\nabla_+ E_+|^2 \exp\left[-\left(\frac{\omega - 2\Omega}{k_{||}v_{th}} \right)^2 \right] \right) \quad (1)$$

where $E_+ = E_n + iE_b$, $\nabla_+ = \nabla_n + i\nabla_b$, and ϵ_0 is the permittivity of free space, ω_p the plasma frequency, $\rho_L^2 = v_{th}^2/2\Omega^2$ the Larmor radius, v_{th} the thermal velocity. Because there are two degrees of freedom in toroidal geometry and several interacting wave branches, the net power flux cannot be defined in general for wavefields with a substantial amount of reflections. In this form, the code describes the propagation, damping and mode conversion of global fast and slow waves in a tokamak plasma. Note that no extra "viscous damping" is added to damp out artificially short wavelength modes, all the power being here absorbed by the physical resonant Landau, cyclotron and TTMP interactions.

Because mode-conversion is in the ICRF a two-dimensional gyrokinetic problem, it is clear that only the last model is formally applicable, in the sense that the gyrokinetic

toroidal solution can only be obtained with a singular perturbation from the fluid-toroidal or gyrokinetic-slab wave equations. In the coming section, the three codes are used to analyze carefully the mode-conversion and point out the differences between models that are often used in the literature.

3 TOROIDAL MODE-CONVERSION

To be able to later compare the calculations with experimental measurements, a mode-conversion scenario is chosen with the parameters of table 1 typical of the DIII-D tokamak. The double-null magnetic field configuration of the discharge 89017 at 1830 msec is reconstructed in toroidal geometry [37, 46] by limiting the outermost flux surface to $q_{edge} = 15$ and in slab geometry by using the approximation $B(x) = B_0 R_0/(R_0 + x)$ in terms of the toroidal magnetic field only. The shape of the vacuum vessel is taken into account exactly in PENN and is modeled with a conducting wall located at constant 20 cm from the plasma in the other two codes. An oscillating antenna current is driven in the vacuum region half way between the plasma edge and the vessel, either on the high (HFS) or low magnetic field side (LFS) of the torus.

With this set-up, the cyclotron layers $\omega = \Omega_H = 2\Omega_D$ intersect the mid-plane on the LFS of the magnetic axis at a normalized radius $s = \sqrt{\psi_n} \simeq 0.25$ (where ψ_n stands for the normalized poloidal magnetic flux), equivalent in slab geometry to the absolute coordinate $x = +10$ cm. Depending on the relative concentration of the ions, Alfvén resonances and ion-ion hybrid resonance-cut-off pairs are formed on the HFS of the cyclotron layers where the dispersion relations $k_{||}^2 = \epsilon_\perp \omega^2/c^2 = \omega^2/c_A^2$ and $\Omega_{DH} \simeq \sqrt{(\omega_D^2\Omega_H^2 + \omega_H^2\Omega_D^2)/(\omega_D^2 + \omega_H^2)}$ are satisfied with $k_{||} = (n + m/q)/R$, $c_A = B/(4\pi \sum n_i m_i)$, $\epsilon_\perp = 1 + \sum \omega_i^2/(\Omega_i^2 - \omega^2)$, where ω_i and Ω_i stand for the plasma and cyclotron frequencies of the species with index i. These resonances are layers where the Alfvén wave propagates along the magnetic field lines: in the lukewarm LION model, they provide for a resonant absorption of the shear-Alfvén wave which depends artificially on the species temperatures and they coincide in gyrokinetic models with the locations where mode-conversion is expected to take place to the kinetic Alfvén wave. Ion-Bernstein waves may also be excited non-resonantly near the layer where $\omega = 2\Omega_D$ and require a gyrokinetic modeling.

3.1 Low field side antenna

Let us begin this study with a plasma composed of 67% deuterium and 34% hydrogen. Using the gyrokinetic slab ISMENE code, fig.1(a) shows how the fast wave emitted on the LFS by an antenna at $x = +70$ cm propagates inwards past the cyclotron layers $\omega = \Omega_H = 2\Omega_D$ at $x = +10$ cm and reaches the cut-off $x \in [-24; -19]$ cm in front of the fast wave ion-ion hybrid resonance where $k_{||}^2 = \epsilon_\perp \omega^2/c^2$. Although a part is reflected, a fraction of the wave power tunnels through to the hybrid resonance at $x = -24$ cm, where the sharp variation of the fast wavefield induces a mode-conversion to the slow wave propagating further to the HFS with a short wavelength until it is completely damped. Resonant wave-particle interactions are responsible for the absorption of the wave energy and lead to the plasma heating. The electron Landau damping (ELD) of the fast wave increases towards the core where the temperature is largest and absorbs already 40% of the total power between the plasma edge and the resonances $\omega = \Omega_H = 2\Omega_D$. The

cyclotron damping by hydrogen and deuterium ions absorb another 6 and 12 % in the interval $x \in [3;17]$ cm, so that only $\sim$ 16% of the total power is finally converted and deposited by slow wave ELD in the interval $x \in [-45;-25]$ cm, the rest being absorbed by fast wave ELD. Fig.1(b) shows the power deposition integrated from the center for each species, assimilating the radial variable with a normalized position $s = |x/60|$ to compare this slab calculation with the toroidal results below.

Even if the fast wavefield in fig.1(c) calculated using the fluid toroidal LION code looks similar in the mid-plane to the prediction from ISMENE, the power deposition in fig.1(b) is in LION entirely dominated by the cyclotron damping from the hydrogen ions. The standing fast wavefield tunnels to the HFS all along the cut-off layer and hits the shear-Alfvén resonances which become clearly visible in fig.1(c); the strong peaking of the resonance wavefield near the cyclotron layer at $\omega = \Omega_H$ is then responsible for up to 85% of the total power absorption. Because the variation of $\epsilon_\perp$ is large along the magnetic surfaces, the shear-Alfvén wave described with the fluid model propagates along the magnetic field with an increasing $k_{||}$ and may get partly reflected or absorbed because the numerical resolution becomes insufficient in the poloidal direction. Toroidal effects are clearly important and explain the large difference between the predictions from ISMENE and LION. Unfortunately, the partition among the species and the deposition profile of the resonantly absorbed power is meaningless, because Budden's resonance absorption [7] does not properly evaluate the power mode-converted in toroidal geometry [21, 23].

A consistent description of the mode-conversion in the tokamak can be obtained with a gyrokinetic toroidal calculation describing the propagation and damping of the mode converted wave: fig.1(d) shows that the result obtained from the PENN code is considerably different from the two previous models. In the background, a global fast wavefield (very similar to the one in LION, but not apparent in the figure) carries the wave power to the HFS of the torus and to the ion-ion hybrid resonance $k_{||}^2 = \epsilon_\perp \omega^2/c^2$; in the neighborhood, mode-conversion induces slow wavefield structures with wavelengths that are similar to those obtained above using ISMENE. The amplitudes compared with the fast wave are however much larger here because standing slow waves form spatially localized eigenmodes that are weakly damped by ELD. Some time ago, localized shear-Alfvén structures have been proposed [47, 48], resulting from the toroidal coupling in regions where $\epsilon_\perp \simeq 0$ and where the wavelength $\lambda_{||} = 2\pi c/(\omega\sqrt{\epsilon})$ matches the characteristic inhomogeneity length along the magnetic field $L = 2\pi Rq$ at relatively high frequencies ω. The more elaborate global wavefield calculation using LION in fig.1(c) clearly shows that such structures are heavily damped and do not emerge from the continuum; this has however to be taken with caution since fluid models are sufficient to describe neither the conversion nor the subsequent damping of the wave forming the eigenmodes. The comprehensive gyrokinetic calculation in fig.1(d) here shows for the first time that relatively weakly damped spatially localized eigenmodes do indeed exist and have a finite radial extension because of the gyro-motion of the ions. Driven to relatively large amplitudes by the ICRF antennas, they may therefore interact relatively well with fast particles and could provide a useful mean to enhance radial transport associated with fusion-born $\alpha-$particles.

3.2 High field side antenna

It is well known that in the plane slab model there is a great difference in the mode-conversion efficiency depending on whether a fast wave is lanched from the high or low

field side of the resonance cut-off pair. Fig.2(a) shows that with ISMENE the fast wave launched from the HFS at $x = -70$ cm propagates inwards and hits the hybrid resonance $k_{\|}^2 = \epsilon_{\perp}\omega^2/c^2$ at $x = -24$ cm, before it gets significatively affected by the ELD. The mode-converted slow wave propagates backwards to the HFS and deposits nearly 100% of the power by ELD in the interval $x \in [-45; -25]$ cm, the transmission through the evanescent layer $x \in [-24; -19]$ cm remaining negligibly small. A similar behavior is also apparent in the LION calculation in fig.2(c), where the fast wave hits directly the shear-Alfvén wave resonances from the HFS, carrying the power to the cyclotron layer $\omega = \Omega_H$ and dissipating up to 93% with resonance absorption through cyclotron damping on the hydrogen ions. The gyrokinetic toroidal result obtained with PENN in fig.2(d) is remarkably similar to fig.1(d), consistent with the weakly damped eigenmode character of the wavefield independent of the antenna position.

The power deposition calculated with fluid LION code in fig.2(b) suggests that most of the power is absorbed by resonance absorption on the hydrogen ions, but can again not be trusted because a fluid modeling is not sufficient. The profiles obtained using the gyrokinetic ISMENE and PENN codes are rather similar and show that contrary to the fluid prediction, nearly 100% of the power is deposited by slow wave ELD in the neighborhood of the ion-ion hybrid resonance $s \in [0.45; 0.65]$. The toroidal deposition profile is radially more localized because of the formation of slow wave eigenmodes which do not at all exist in the slab model; plotting the local power deposition throughout the cross-section makes it clear that the power is absorbed away from the mid-plane, in the regions where the electric field in fig.1(d) and 2(d) is large in average, underlining the qualitative difference behind the results which look similar in the slab and in the toroidal geometry.

3.3 Dependence on the equilibrium parameters

From the local wave propagation theory, it is known that when the deuterium density fraction $n_D/(n_H + n_D)$ is raised from 0 to 1, the mode-converted wave changes from a kinetic Alfvén wave induced at Alfvén resonances on the HFS of $\omega = \Omega_H$, to a slow wave propagating in the neighborhood of the ion-ion hybrid resonance $k_{\|}^2 = \epsilon_{\perp}\omega^2/c^2$, becoming finally an ion-Bernstein wave propagating on the HFS of $\omega = 2\Omega_D$ in a pure deuterium plasma.

Fig.3 shows the global wavefield obtained using the gyrokinetic toroidal PENN code in the ion-ion hybrid regime using a LFS antenna and equal ion densities $n_H = n_D$. Compared with the previous scenario in fig.1(d), the ion-ion hybrid resonance is here slightly shifted to the HFS; the main difference however comes from the parameters which do not any longer exactly match those of the slow wave eigenmode. The background wavefield gaining in relative amplitude becomes more visible on the plot, with a long wavelength partially standing fast wavefield that peaks at the hybrid resonance and generates a slow wave with nearly vertical wavefronts in the mid-plane. Away from the mid-plane, the Alfvénic character of the slow wave makes the short-wavelength oscillations follow the magnetic field lines and propagate counter-clockwise along the flux surfaces. A contribution from the former slow eigenmode wavefield subsists in the region where $\epsilon_{\perp} \simeq 0$ and a new short wavelength oscillation also appears in the neighborhood of $\omega = 2\Omega_D$ which is identified as an ion-Bernstein wave. Up to 82% of the power is in this scenario de-

posited by the slow wave ELD away from the axis around $s = 0.6$, cyclotron interactions absorbing the rest of the power with 15% on hydrogen and 3% on deuterium ions.

Reducing the deuterium content down to 12% and below brings the hybrid resonance ever closer to the cyclotron layer at $\omega = \Omega_H$. The mode-converted slow wave (here poorly resolved with the mesh in the upper half-plane of fig.4) gets increasingly damped by the resonant cyclotron interactions absorbing the majority of the power until the slow wave disappears completely in presence of a couple of percent deuterium only. On the HFS of the ion-ion hybrid resonance, mode conversion becomes most effective at the outermost Alfvén resonance where the electron temperature is large enough to satisfy $\omega/(k_{||}v_e) < 1$ [23]; it generates a flux surface aligned Alfvénic wave that escapes radially inwards from the region where it cannot anymore follow the magnetic field lines counter-clockwise across the cyclotron layer (lower half-plane in fig.4).

If the deuterium concentration is on the contrary raised to 88% and above, the ion-ion hybrid layer is completely removed from the plasma on the HFS of the torus. Fig.5 shows that the mode-conversion remains nevertheless possible by toroidal coupling of the slow wave in the region where $\epsilon_\perp \simeq 0$, leading to an off-axis power deposition by slow wave ELD around $s = 0.6$. Above 96%, the mode-conversion to ion-Bernstein waves along the cyclotron layer $\omega = 2\Omega_D$ becomes dominant and deposits the power on the different species in the same manner as previously shown for JET in Ref.[40]. The temperature being lower here, it is not possible to resolve well enough the short wavelengths associated with the ion-Bernstein wave.

Varying parameters other than the relative ion concentration, such as the magnetic field and the species temperature does of course affect the propagation, the damping and the mode-conversion of the fast and slow waves, but does not significatively change the qualitative description given above.

4 DISCUSSION AND SUMMARY

From the abundance of different mode-conversion regions and the diversity of the underlying physical mechanisms, it appears clearly that a reliable prediction of the mode-converted power requires at least a global gyrokinetic toroidal calculation, taking into account the propagation and the damping of the slow wave. Apart from the parallel electric field which has here been taken into account, the main difference between the results obtained using PENN and the predictions from other codes [26] is mainly due to the discretization in real space, which allows for a description of wavefields that are poloidally very localized without having to deal with very broad Fourier spectra which can only be resolved with great difficulty. The price to pay for this reduction from an integral to a partial-differential equation is of course the functional approximation of the parallel wave vector, evaluating the resonant wave-particle interaction without the poloidal mode number in the second term of the operator $k_{||} = (n + m/q)/R$. Using the iterative procedure in eqs.52-53 of Ref.[23], it is however possible to check a posteriori how good the approximation $k_{||}^{(0)} = n/R$ is. In most of the cases (and in all the figures of this paper), the wavefield does not change significatively when iterating, simply because the slow waves in the ICRF have the tendency to develop wavelengths that are much shorter radially than poloidally so that the condition $n > m/q$ is often satisfied.

To summarize, ICRF mode-conversion has for the first time been numerically resolved

in tokamak geometry, showing where the slow wave is born, how it propagates, gets reflected and damped by resonant wave-particle interactions. Different mode-conversion regions have been identified, such as the outermost Alfvén resonance where $\omega/(k_{\|}v_e) < 1$ on the HFS of the lowest frequency cyclotron layer, the region where $\epsilon_{\perp} \simeq 0$, the ion-ion hybrid resonance and the ion-Bernstein cut-off along the second harmonic cyclotron layer. Relatively weakly damped slow wave eigenmodes are formed by toroidal coupling where $\epsilon_{\perp} \simeq 0$; in a scenario where the fast wave damping is relatively weak, they yield a power deposition which is independent of the antenna location and could in a reactor be driven to sufficiently large amplitudes so as to interact efficiently with fast particles.

Acknowledgments

Useful discussions with K.Appert, O.Sauter, L.Villard and J.Vaclavik are gratefully acknowledged. The linear wave propagation codes ISMENE, LION and PENN have all been developed at CRPP Lausanne. This work was supported in part by the Swedish, the Swiss National Science Foundations and the super-computer center in Linköping.

List of Figures

Table 1: Parameters for a mode-conversion scenario in DIII-D.

major radius	R_0	1.96 m
magnetic field	B_0	2.14 Tesla
safety factor (axis, edge)	$q_0 - q_{edge}$	$2 - 15$
volume averaged pressure	$< \beta >$	1.0 %
antenna frequency	f_{ant}	31 MHz
poloidal antenna extension	θ_{ant}	52 deg.
toroidal wave vector	$k_\varphi = n/R$	10.2 m^{-1}
density $n_e = n_D + n_H = n_0(1 - 0.95s^2)^{0.8}$	n_0	4.5×10^{19} m^{-3}
temperature $T_e = T_{e,0}(1 - 0.95s^2)$	$T_{e,0}$	2 keV
$T_D = T_H = T_{i,0}(1 - 0.95s^2)$	$T_{i,0}$	1.5 keV
discretization ISMENE cubic FEM	N_x	800
LION bi-linear hybrid FEM	$N_{rad} \times N_{pol}$	200×140
PENN bi-cubic FEM	$(N_{rad} + N_{rad}^{vac}) \times N_{pol}$	$(100 + 12) \times 100$

References

[1] F.PERKINS, Nucl. Fusion **17** (1977) 1197

[2] N.J.FISCH, Phys. Plasmas **2** (1995) 2375

[3] R.MAJESKI *et al.*, Phys. Rev. Lett. **76** (1996) 764

[4] B.SAOUTIC *et al.*, Phys. Rev. Lett. **76** (1996) 1647

[5] T.INTRATOR *et al.*, Phys. Plasmas **3** (1996) 1331

[6] P.BONOLI *et al.*, *MIT report* PFC/JA-96-48, submitted to Phys. Plasmas

[7] K.BUDDEN, *Radio Waves in the Ionosphere*, Cambridge University Press (1961)

[8] D.G.SWANSON, Phys. Fluids **24** (1981) 2035

[9] T.H.STIX, *Waves in Plasmas*, American Institute of Physics (1992)

[10] M.BRAMBILLA, A.CARDINALI, Plasma Phys. **10** (1982) 1187

[11] P.COLESTOCK, R.KASHUBA, Nucl. Fusion **23** (1983) 763

[12] T.HELLSTEN *et al.*, Nucl. Fusion **25** (1985) 99

[13] K.APPERT *et al.*, Comput. Phys. Commun. **40** (1986) 73

[14] J.Vaclavik, K.Appert, *Nucl.Fusion* **31** (1991) 1945

[15] M.BRAMBILLA, Nucl. Fusion **28** (1988) 549

[16] M.ONO, Phys. Fluids B **5** (1993) 241

[17] O.SAUTER, J.VACLAVIK, Comput. Phys. Commun **84** (1994) 226

[18] D.GAMBIER, A.SAMAIN, Nucl. Fusion **25** (1985) 283

[19] L.VILLARD *et al.*, Comput.Phys.Reports **4** (1986) 95

[20] E.JAEGER *et al.*, Nucl. Fusion **33** (1993) 179

[21] K.APPERT *et al.*, Plasma Phys. Contr. Fusion **30** (1988) 1195

[22] A.JAUN *et al.*, *On the Validity of Resonance Absorption and Continuum Damping*, to be submitted to Plasma Phys. Contr. Fusion (1997)

[23] A.JAUN *et al.*, Comput. Phys. Commun. **92** (1995) 153

[24] K.ITOH *et al.*, Nucl. Fusion **24** (1984) 224

[25] A.FUKUYAMA *et al.*, Comput. Phys. Reports **4** (1986) 137

[26] M.BRAMBILLA, T.KRUCKEN, Nucl. Fusion **28** (1988) 1813

[27] A.HASEGAWA, L.CHEN, Phys. Rev. Lett. **35** (1975) 370

[28] V.GOLANT, Soviet Phys. Tech. Phys. **16** (1972) 1980

[29] T.STIX, Phys. Rev. Lett. **15** (1965) 878

[30] A.JAUN *et al.*, Plasma Phys. Contr. Fusion **39** (1997) 549

[31] A.JAUN *et al.*, *Prediction of Alfvén Eigenmode Dampings in JET*, submitted to Phys. Plasmas (1997)

[32] T.HELLSTEN, E.TENNFORS, Physica Scripta **30** (1984) 341

[33] TH.MARTIN, J.VACLAVIK, Helv. Phys. Acta **60** (1987) 471

[34] B.McVEY *et al.*, Phys. Rev. Lett. **55** (1985) 507

[35] J.VACLAVIK, K.APPERT, Plasma Phys. Contr. Fusion **29** (1987) 257

[36] A.JAUN *et al.*, Plasma Phys. Contr. Fusion **33** (1991) 521

[37] H.LUTJENS *et al.*, Comput. Phys. Commun. **97** (1996) 219

[38] X.LLOBET *et al.*, in proc. Joint Varenna-Lausanne Int. Workshop Chexbres (1988) 663

[39] A.JAUN *et al.*, Phys. Plasmas **4** (1997) 1110

[40] A.JAUN *et al.*, *Ion-Bernstein Wave Mode-Conversion in a Hot Tokamak Plasma*, in proc. 12th Topical Conf. on RF Power in Plasmas, Savannah, AIP (1997)

[41] W.W.Heidbrink *et al.*, *Stable Ellipticity-Induced Alfvén Eigenmode in JET*, Accepted in Phys. Plasmas (1997)

[42] D.B.BATCHELOR *et al.*, in proc. Joint Varenna-Lausanne Int. Workshop Chexbres (1988) 691

[43] S.BRUNNER, J.VACLAVIK, Phys. Fluids B **5** (1993) 1695

[44] L.VILLARD *et al.*, Nucl. Fusion **35** (1995) 1173

[45] J.Vaclavik, *Private Communication* (1996)

[46] L.L.LAO *et al.*, Nucl. Fusion **30** (1990) 1035

[47] B.COPPI *et al.*, Phys. Fluids **12** (1986) 4060

[48] V.MOISEENKO, in proc. 21st EPS Conference on Controlled Fusion and Plasma Physics, Montpellier (1994), Europhysics Conference Abstracts Vol.18 B I p.50

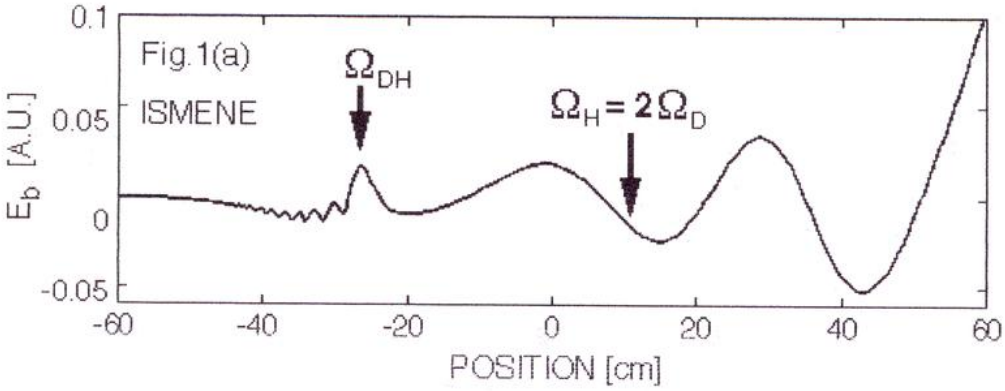

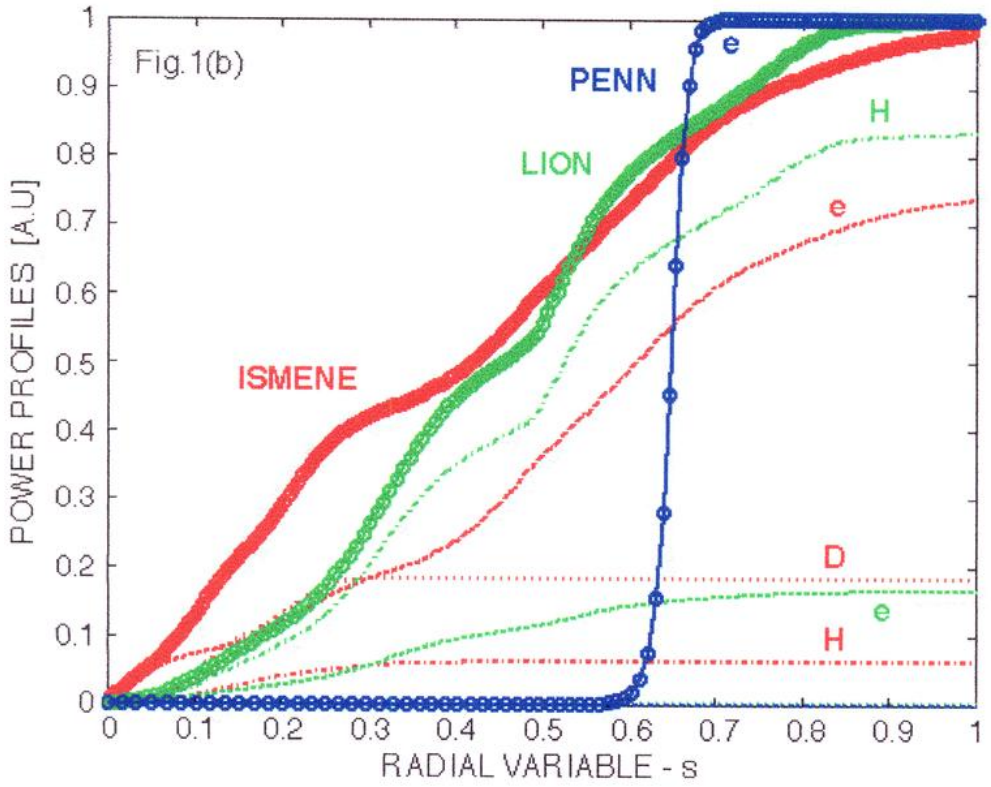

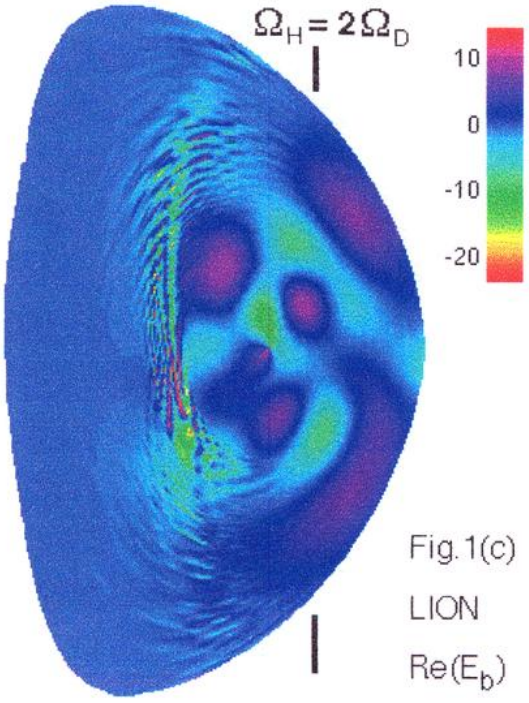

Fig.1(c)
LION
$Re(E_b)$

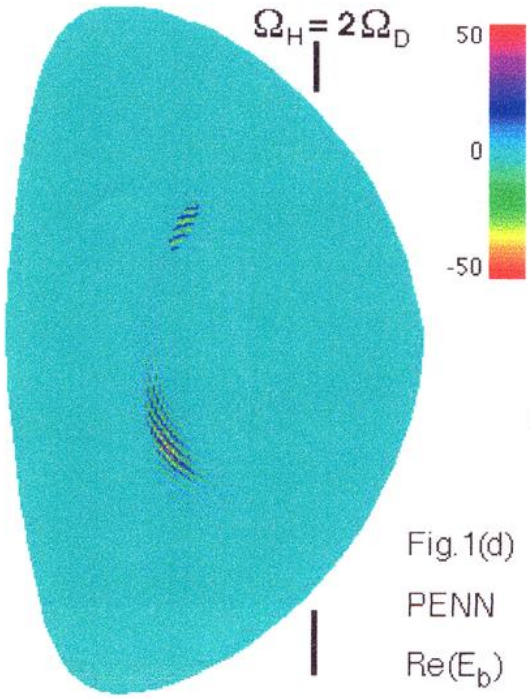

Fig.1(d)
PENN
$Re(E_b)$

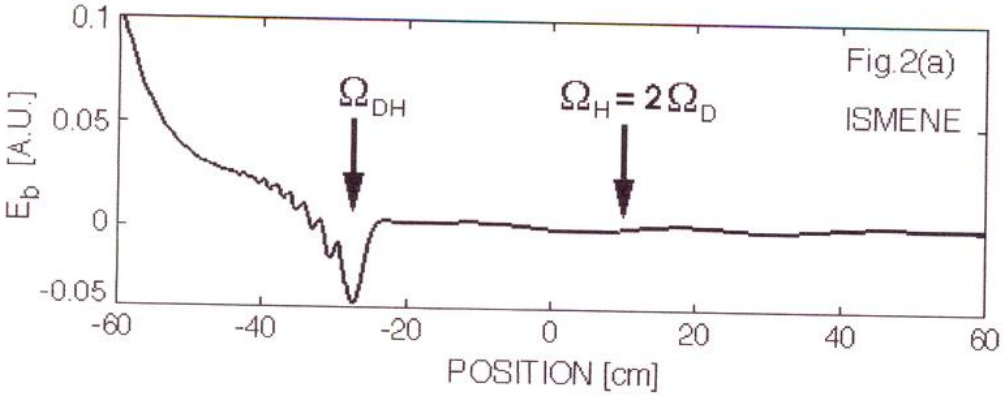

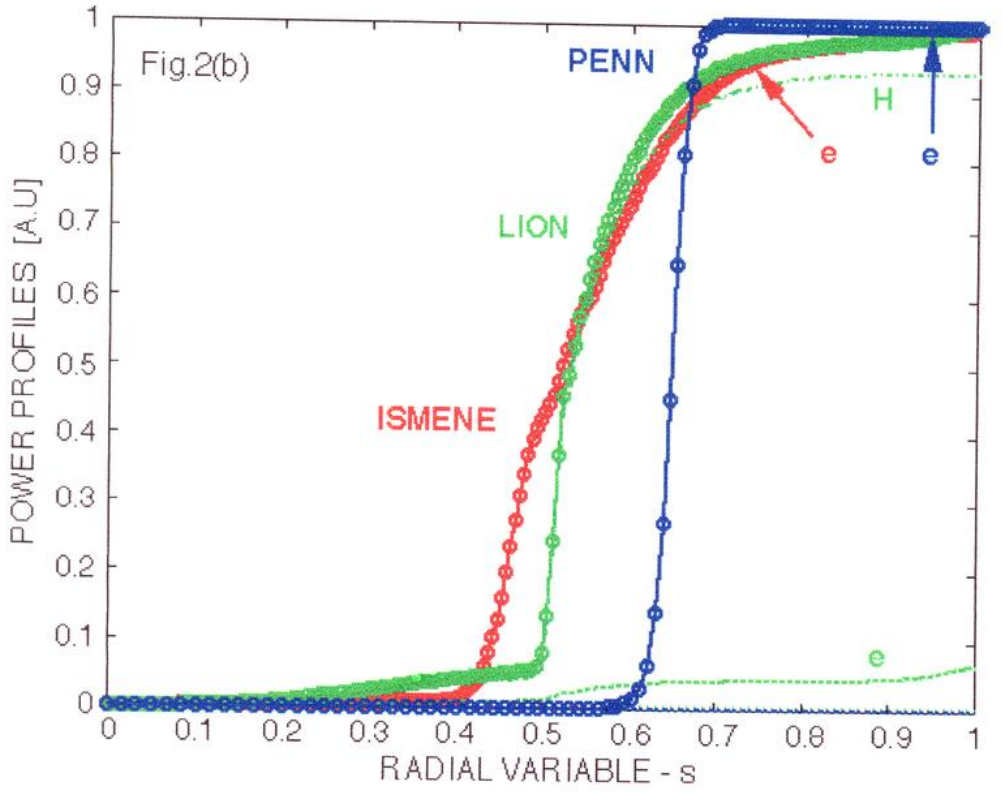

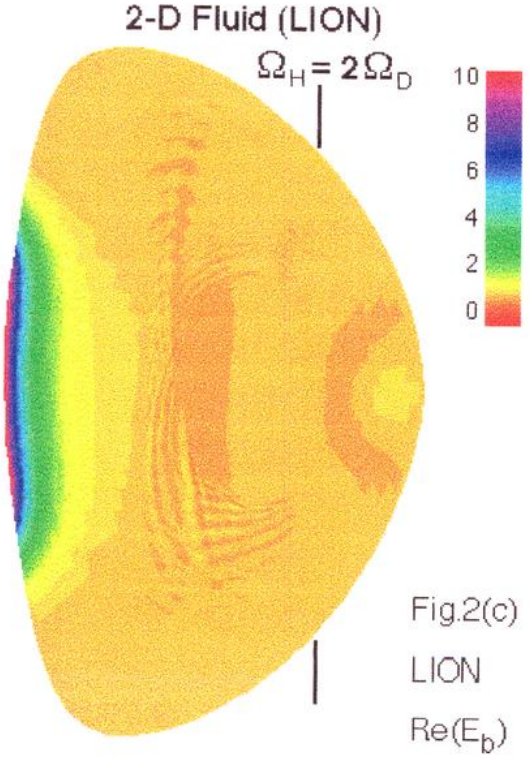

Fig.2(c)
LION
$Re(E_b)$

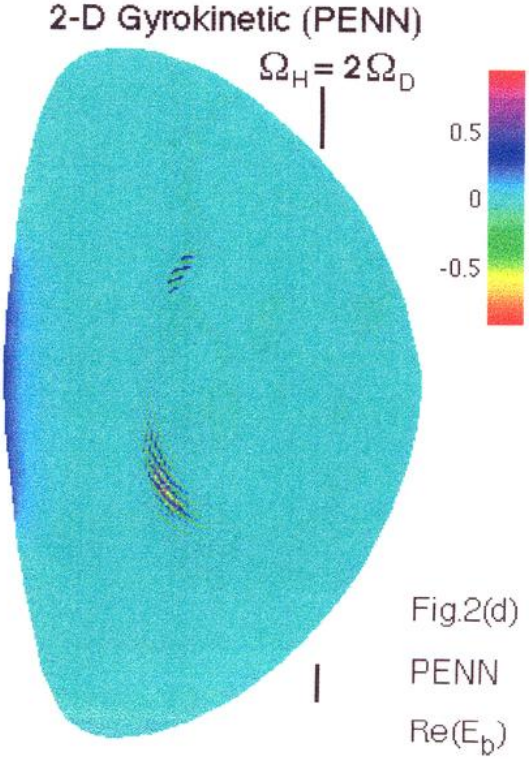

Fig.2(d)
PENN
$Re(E_b)$

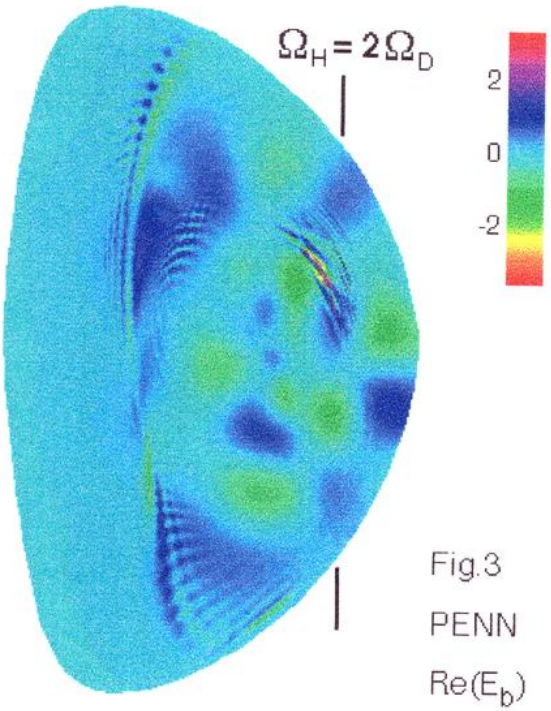

Fig.3
PENN
$Re(E_b)$

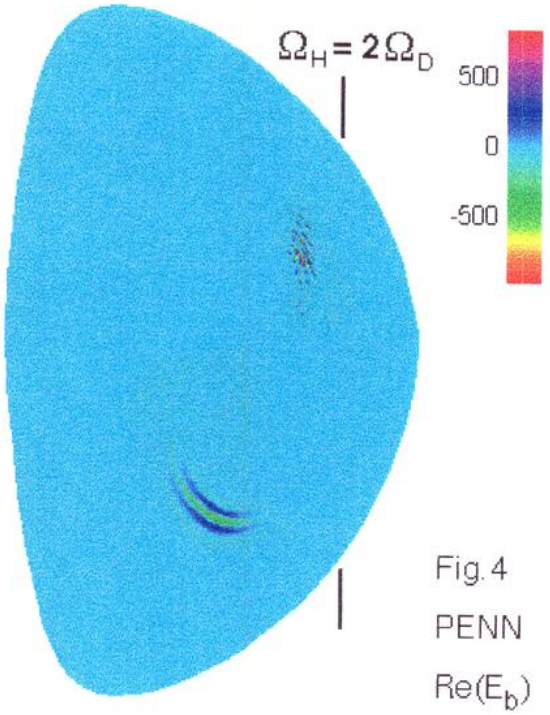

Fig.4
PENN
$Re(E_b)$

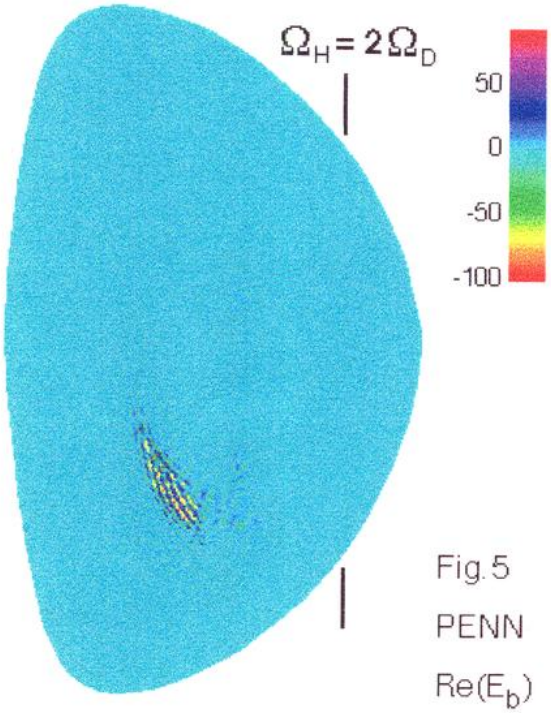

Fig.5
PENN
$Re(E_b)$

ANNEX:

Ion-Bernstein Wave Mode Conversion in Hot Tokamak Plasmas

A. Jaun[1], T. Hellsten[1], S. C. Chiu[2]

[1] *Alfvén Laboratory, EURATOM-NFR Association, KTH, 100 44 Stockholm, Sweden*

[2] *General Atomics, San Diego, California 92186-9784, USA*

Abstract. Mode conversion at the second harmonic cyclotron resonance is studied in a toroidal plasma, showing how the ion-Bernstein wave can dramatically affect the power profile and partition among the species. The results obtained with the gyrokinetic toroidal PENN code in particular suggest that off-axis electron and second harmonic core ion heating should become important when the temperatures in JET reach 10 keV.

INTRODUCTION

Several waves often propagate in a plasma at a fixed frequency, but they usually do not interact because they have very different wavelengths. Where the spatial scale of two waves match, the power associated with one branch may however be transferred to the other in a process called linear mode conversion. It generally takes place in the vicinity of resonances where the spatial scale of the fast wave gets shorter or cut-offs where the scale of the slow wave gets longuer [1], but can also occur at a confluence [2] or be induced by toroidal coupling [3].

In this paper, mode conversion between the fast wave (FW) and the slow ion-Bernstein wave (IBW) is studied at the second harmonic cyclotron resonance, taking into account the specific geometry of the tokamak. It has previously been shown in ref.[4] that the power mode converted to Alfvén waves in a torus cannot simply be calculated with fluid plasma models using resonance absorption [5]; since IBW mode conversion takes place at a slow wave evanescence without a fluid resonance present at all, it is clear that the results will also be very different from toroidal fluid models.

MODEL

To model the wave propagation in a hot tokamak, the gyrokinetic toroidal PENN code [4] solves Maxwell's equations in real space using a bi-cubic finite elements representation of the electromagnetic potentials $(A_n, A_b, A_{||}, \phi)$ avoiding "numerical pollution". A Grad-Shafranov equilibrium [6] defines the plasma response using a second order Larmor radius expansion of the dielectric tensor [7]. The velocity integrals over the resonant denominators $(\omega - l\Omega - k_{||}v_{||})^{-1}$ are

evaluated assuming an approximate functional dependence $k_{||} = n/R$ instead of using the exact operator $k_{||} = -iB^{-1} \vec{B} \cdot \nabla$, where ω stands for the frequency, $l\Omega$ a multiple of the cyclotron harmonic, n the toroidal mode number, R the major radius and $k_{||}$ the wave-vector along the local magnetic field $\vec{B}$. The power absorption through electron Landau damping and transit-time magnetic pumping (TTMP) is evaluated in the drift-kinetic approximation with the formulas 50-51 of ref.[8], and completed with the first and second harmonic ion cyclotron absorption [9]:

$$P_c = \sqrt{\pi}\epsilon_0 \int d^3x \frac{\omega_p^2}{4|k_{||}|v_{th}} \left(|E_+|^2 \exp\left[-\left(\frac{\omega - \Omega}{k_{||} v_{th}} \right)^2 \right] + \rho_L^2 |\nabla_+ E_+|^2 \exp\left[-\left(\frac{\omega - 2\Omega}{k_{||} v_{th}} \right)^2 \right] \right)$$

where $E_+ = E_n + iE_b$, $\nabla_+ = \nabla_n + i\nabla_b$, and ϵ_0 is the permittivity of free space, ω_p the plasma frequency, $\rho_L^2 = v_{th}^2/2\Omega^2$ the Larmor radius, v_{th} the thermal velocity. In this form, the code describes the propagation, damping and mode conversion of global fast and slow waves in a tokamak, with a power absorption occurring through resonant Landau, cyclotron and TTMP interactions.

RESULTS

An up-down symmetric deuterium plasma with a low hydrogen concentration is used with the parameters of fig.1. Driving an oscillating antenna current in the low magnetic field side (LFS) vacuum region of the torus, the frequency ω is adjusted so that the cyclotron resonances $\Omega_H = 2\Omega_D$ intersect the mid-plane near the magnetic axis (dashed line in fig.1a-c). Raising the bulk plasma temperature $T = T_e = T_D$ while keeping all other parameters fixed, global wavefields and power deposition profiles are computed with the gyrokinetic PENN [4] and the fluid LION [10] codes.

When the bulk temperature is as low as 200 eV, fig.1a shows that the FW emitted on the LFS is first focused to the magnetic axis, where it is damped by the hydrogen minority cyclotron interactions. Mode conversion is absent, the electron Landau, TTMP and second harmonic deuterium absorptions are all negligible, and both codes agree fairly well as can be seen from the integrated total power $P(s) = \int_{V(s')} P(s', \theta) dV(s', \theta)$ in fig.1d, where $s = \sqrt{\psi}$ refers to the normalized radius and θ to the poloidal angle.

Raising the bulk temperature to 2 keV results in a dramatic change of the wavefield structure: fig.1b shows how mode conversion occurs on the high magnetic field side of the resonance $2\Omega_D$ around $s = 0.25$, with a relatively short wavelength $k_\perp \rho_D < 0.2$ ion-Bernstein wave propagating outwards until it gets reflected at $s \simeq 0.8$. The FW field in the background (barely visible on the plot) remains almost unchanged, which is in agreement with the result obtained from the fluid LION code and explains why the total power profile from LION in fig.1e is only weakly affected by the temperature rise. The mode conversion taking place

in the gyrokinetic wavefield however modifies that profile, with the hydrogen minority absorption getting localized around the mode conversion surface due to the IBW polarization $E_+/E \simeq 0.5$, which is more favourable for resonant interactions at $\omega = \Omega_H$ than the FW (first term in P_c). The IBW propagates away with a finite parallel electric field $E_\parallel/E \simeq 0.005$ and deposits a small fraction of the power directly on the electrons through Landau damping.

When the bulk temperature is increased to 10 keV in the core, IBW mode conversion becomes possible further outside: two distinct layers appear in fig.1c at $s \simeq 0.3, 0.6$ where the fast and the slow wave locally match with different poloidal mode numbers. The IBW propagates along the HFS of the resonance $2\Omega_D$, and due to relatively long poloidal evanescence length, extends also somewhat to the LFS of it. The gyrokinetic power profile in fig.1f is then totally different from the fluid prediction, with power absorption due mainly to electrons Landau damping of the IBW at the mode conversion layers, and around $s \simeq 0.3$ due to second harmonic cyclotron interaction with the majority deuterons (second term in P_c). The latter here dominates over the minority hydrogen absorption because of the low hydrogen concentration and the short wavelength $k_\perp \rho_D \simeq 0.5$ of the IBW, still just within the validity limits of the finite Larmor radius expansion [11].

In principle, it is possible to model the scenarios of fig.1 in slab geometry and compute the wavefield for an imposed poloidal mode number. The mode conversion is then homogeneous along the HFS of the resonance $2\Omega_D$, and the IBW propagates away from it horizontally. The toroidal calculations in fig.1 however show that the mode conversion is far from homogeneous and that the IBW needs not in general to propagate away from the resonance. When it is on the contrary approaching it, strong cyclotron interactions occur with the ions, resulting in a heating mechanism which is really a combination of gyrokinetic and toroidal effects.

CONCLUSION

Mode conversion between the fast and the IBW has been studied in a tokamak. The results show that the power deposition calculated for a warm plasma using fluid plasma models is misleading and that a gyrokinetic model is necessary to take the conversion into account. While it has only little effect for low temperatures, the mode conversion modifies dramatically the power profile and the partition among the species when the temperatures get as high as in the tokamaks nowadays. In particular, the PENN code predicts that strong off axis electron heating and second harmonic core ion heating should take place in 10 keV JET-like deuterium plasmas with a low hydrogen concentration.

Useful discussions with J.Vaclavik are gratefully acknowledged. The linear wave propagation code LION and PENN have been developed at CRPP Lausanne. This work was supported in part by the Swedish National Science Foundation and the computer center in Linköping.

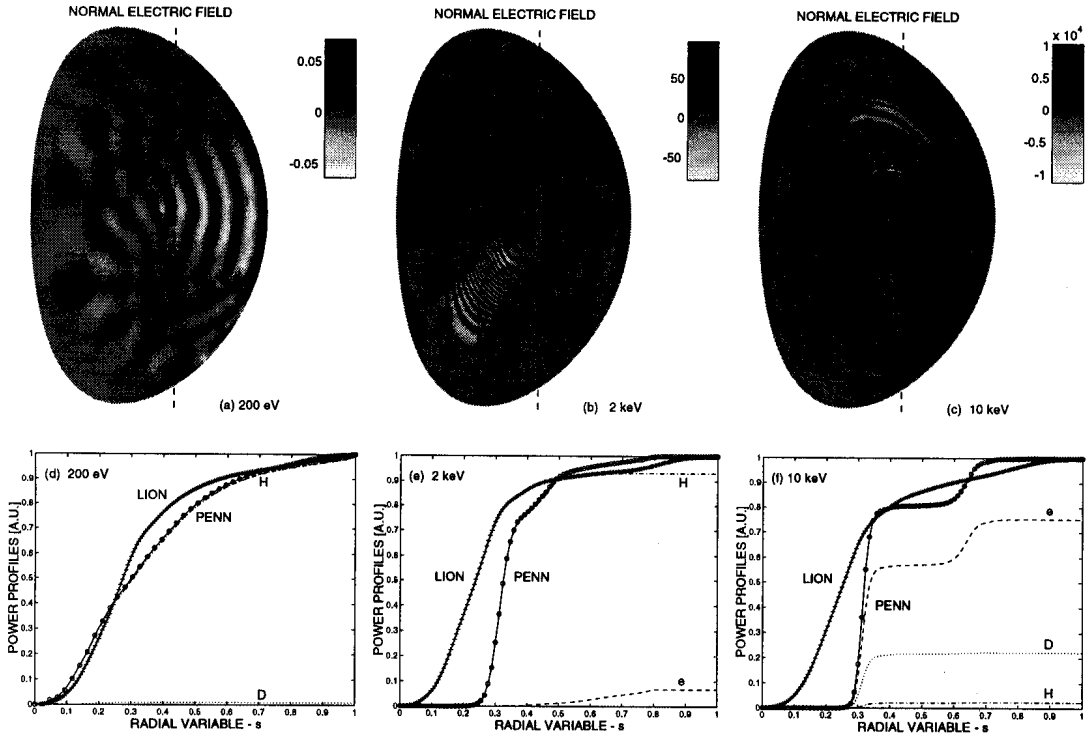

Figure 1: Normal electric field amplitude $\Re e(E_n)$ obtained with the gyrokinetic PENN code (a-c) for an increasing bulk temperature $T_e = T_D = T(1 - 0.9s^2)$; in (d-f) the corresponding total power absorption profiles (circles) are compared with the fluid LION code (crosses). The kinetic power fractions correspond to power absorbed by the electrons (dashes), minority H-ions (dash-dots) and majority deuterons (dots). The parameters are those of a JET discharge driven with an antenna at 33 MHz with $n_{tor} = 25$ and an equilibrium $B_T = 2.17$ T, $q_0 = 1.03$, $q_a = 2.4$, $n_D = 3(1 - 0.9s^2)^{0.55}10^{19}m^{-3}$, $n_H/n_D = 0.04$, $T_H = 10(1 - 0.9s^2)$ keV.

REFERENCES

[1] T.H.Stix, *Waves in Plasmas*, American Institute of Physics (1992)
[2] V.Golant, Soviet Phys.Tech.Phys. **16** (1972) 1980
[3] A.Jaun *et al.*, *16th IAEA Fusion Energy Conf.* Montreal 1996
[4] A.Jaun *et al.*, Comput.Phys.Commun. **92** (1995) 153
[5] K.Budden, *Radio Waves in the Ionosphere*, Cambridge University Press (1961)
[6] H.Lütjens, A.Bondeson, O.Sauter, Comput.Phys.Commun. **97** (1996) 219
[7] S.Brunner, J.Vaclavik, Phys.Fluids B **5** (1993) 1695
[8] L.Villard, S.Brunner, J.Vaclavik, Nucl.Fusion **35** (1995) 1173
[9] J.Vaclavik, *Private Communication* (1996)
[10] L.Villard *et al.*, Comput.Phys.Reports **4** (1986) 95
[11] O.Sauter, J.Vaclavik, Nucl. Fusion **32** (1992) 1455